

Large scale polarizability calculations using the approximate coupled cluster model CC2 and MP2 combined with the resolution-of-the-identity approximation

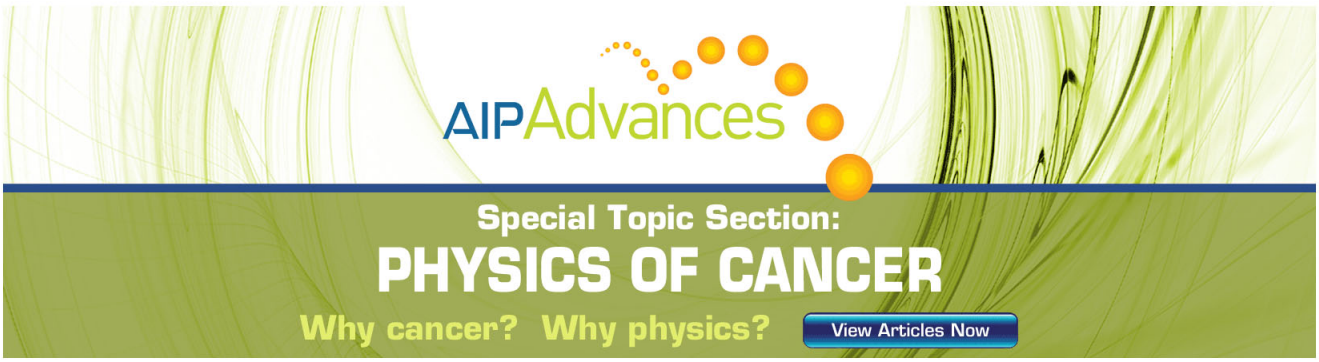
Daniel H. Friese, Nina O. C. Winter, Patrick Balzerowski, Raffael Schwan, and Christof Hättig

Citation: J. Chem. Phys. **136**, 174106 (2012); doi: 10.1063/1.4704788
View online: http://dx.doi.org/10.1063/1.4704788
View Table of Contents: http://jcp.aip.org/resource/1/JCPSA6/v136/i17
Published by the American Institute of Physics.

Additional information on J. Chem. Phys.

Journal Homepage: http://jcp.aip.org/
Journal Information: http://jcp.aip.org/about/about_the_journal
Top downloads: http://jcp.aip.org/features/most_downloaded
Information for Authors: http://jcp.aip.org/authors

ADVERTISEMENT



Downloaded 21 Sep 2012 to 134.147.252.238. Redistribution subject to AIP license or copyright; see http://jcp.aip.org/about/rights_and_permissions

Large scale polarizability calculations using the approximate coupled cluster model CC2 and MP2 combined with the resolution-of-the-identity approximation

Daniel H. Friese,[a] Nina O. C. Winter, Patrick Balzerowski, Raffael Schwan, and Christof Hättig[b]
Lehrstuhl für Theoretische Chemie, Ruhr-Universität Bochum, D-44801 Bochum, Germany

(Received 29 February 2012; accepted 4 April 2012; published online 2 May 2012)

We present an implementation of static and frequency-dependent polarizabilities for the approximate coupled cluster singles and doubles model CC2 and static polarizabilities for second-order Møller-Plesset perturbation theory. Both are combined with the resolution-of-the-identity approximation for electron repulsion integrals to achieve unprecedented low operation counts, input–output, and disc space demands. To avoid the storage of double excitation amplitudes during the calculation of derivatives of density matrices, we employ in addition a numerical Laplace transformation for orbital energy denominators. It is shown that the error introduced by this approximation is negligible already with a small number of sampling points. Thereby an implementation of second-order one-particle properties is realized, which avoids completely the storage of quantities scaling with the fourth power of the system size. The implementation is tested on a set of organic molecules including large fused aromatic ring systems and the C_{60} fullerene. It is demonstrated that exploiting symmetry and shared memory parallelization, second-order properties for such systems can be evaluated at the CC2 and MP2 level within a few hours of calculation time. As large scale applications, we present results for the 7-, 9-, and 11-ring helicenes. © *2012 American Institute of Physics*. [http://dx.doi.org/10.1063/1.4704788]

I. INTRODUCTION

The calculation of second-order properties for molecules with more than a dozen atoms using correlated wave function methods is still a challenge for quantum chemistry. On the one hand, properties such as vibrational frequencies, polarizabilities, magnetizabilities, etc., are of great interest; on the other hand, their calculation is computationally expensive. Often also numerical approaches are employed to calculate second- and higher-order properties since the development of efficient analytic implementations is technically demanding.[1] However, when it comes to frequency-dependent or magnetic properties or if nearly degenerate states are involved, analytical approaches are substantial. While, in general, density functional theory has proven to be very useful for treating most ground state molecular properties such as vibrational spectra,[2] it performs poorly when it comes to polarizabilities. This was found by van Gisbergen *et al.* for dispersion coefficients which depend on the polarizability.[3] McDowell *et al.*[4] and Champagne *et al.*[5] have pointed out that long-range correlation effects play an important role for the treatment of polarizabilities. For the treatment of large π-systems, Champagne *et al.* argued that the deficiencies of DFT for polarizabilities are due to the "shortsightedness" of the exchange-correlation functionals which only "feel the local density".[5]

This is not only crucial for first-order polarizabilities but also for hyperpolarizabilities. The computationally cheapest correlated wave function methods applicable for the calculation of polarizabilities and other second-order properties are second-order Møller-Plesset perturbation theory (MP2) and in the frequency-dependent case, the approximate coupled cluster singles and doubles model CC2. The CC2 model was introduced by Christiansen *et al.*[6] as an approximation to coupled-cluster singles and doubles (CCSD) and can be used within the framework of coupled-cluster response theory for the computation of excitation energies and frequency-dependent properties. The computational costs for CC2 calculations scale formally as $\mathcal{O}(\mathcal{N}^5)$ with the system size and it provides ground state energies correct through second order in the electron fluctuation potential. In this sense it is comparable to the widely known MP2 method.

The first implementations of static polarizabilities for MP2 have been presented by Handy *et al.*[7,8] Frequency-dependent polarizabilities were reported by Rice and Handy[9] in 1991 and by Hättig and Heß[10] in 1995. A first implementation of CC2 polarizabilities was developed by Christiansen *et al.*[11] in the DALTON program. Gauss *et al.* have reported further implementations of second derivatives for various coupled cluster methods.[12,13] Recently, Korona[14] reported an implementation of frequency-dependent polarizabilities with an extension of the CC2 model denoted by XCC2. This approach is not based on the Lagrangian technique, which will be introduced later in this work, but on the expectation value of the CC2 energy. XCC2 has proven to reproduce the CCSD values of the polarizability quite well.

However, all these implementations use exact four-index electron repulsion integrals (ERIs) and therefore have high

[a]Author to whom correspondence should be addressed. Electronic mail: daniel.friese@ruhr-uni-bochum.de.
[b]christof.haettig@rub.de.

 © 2012 American Institute of Physics

Downloaded 21 Sep 2012 to 134.147.252.238. Redistribution subject to AIP license or copyright; see http://jcp.aip.org/about/rights_and_permissions

computational costs in the time-determining $\mathcal{O}(\mathcal{N}^5)$-scaling steps for the evaluation of the ERIs in the molecular orbital (MO) basis and storage requirements scaling with $\mathcal{O}(\mathcal{N}^4)$. Pedersen *et al.* reported an implementation of second-order one-electron properties at the CC2 level which employed an integral-direct Cholesky decomposition of the four-index ERIs in the atomic orbital (AO) basis to replace the time-determining four-index transformation by a cheap three-index transformation of the decomposed AO integrals followed by a fast matrix-matrix multiplication of the transformed decomposition vectors.[15] With this approach, they could, for the first time, present polarizability results for C_{60} at this level of theory in the aug-cc-pVDZ basis. The Cholesky decomposition requires, however, that the two-electron integrals can be arranged as positive definite matrices, which limits the applicability of this approximation for derivatives with respect to geometrical distortions and magnetic properties with gauge including atomic orbitals (GIAOs).

An alternative approach to reduce the computational costs are local correlation methods which have been tested for polarizability calculations by Korona *et al.* using a finite-field approach.[16] It turned out that orbital-relaxation effects have a high influence on the accuracy of the localization error. This limits the applicability of such approaches to static polarizabilities since orbital-relaxed approaches suffer from an unphysical pole structure in the response of the orbitals which they inherit from the preceding coupled perturbed Hartree-Fock (CPHF) calculation.

The polarizability is the simplest molecular property which corresponds to second derivatives of the molecular energy. Accurate polarizabilities are of special interest for the treatment of non-bonding interactions in general and for the setup of so-called "training sets" for polarizable force fields[17,18] in particular. An implementation of polarizabilities is also an important keystone on the way to other second-order properties such as dipole gradients and force constants, which are needed for the calculation of vibrational spectra, and for magnetizabilities and nuclear magnetic resonance (NMR) chemical shifts.

In the following, we present an implementation of polarizabilities for MP2 and CC2 with the resolution-of-the-identity (RI) approximation, also known as density-fitting (DF). The RI approximation is similar as the Cholesky decomposition an inner projection method to decompose four-index two-electron integrals into three-index intermediates. In difference to the latter, it does, however, not require positive definite integral matrices and it has a somewhat lower prefactor for the AO to MO transformation and integral assembly steps, which are time-determining for MP2 and CC2. In combination with the RI approximation, both methods are very performant and useful for the calculation of a variety of properties for ground states[19] and, in the case of CC2, also for excited states.[20–22] The RI approximation reduces the operation count for setting up the two-electron integrals in the MO basis and allows for algorithms which never have to store any doubles amplitudes during calculations of energies and first derivatives. To completely avoid the storage of any $\mathcal{O}(\mathcal{N}^4)$-scaling arrays also during the evaluation of derivatives of density matrices, we employ in addition a numerical Laplace transformation of orbital energy denominators for double excitation amplitudes. Otherwise calculations on larger molecules would suffer from the enormous storage demands for the amplitudes. E.g., for 9-helicene in the aug-cc-pVTZ basis, which is presented as a large scale application in this paper, storage of all doubles amplitudes and Lagrangian multipliers would require about 640 GB. Several TB of disc space would be needed for the calculation we did on the 11-helicene molecule.

In the following, we will first present an overview of the working equations in Sec. II and briefly discuss the layout of our implementation in Sec. III, before we present the results of benchmark calculations for the accuracy and the performance of the implementation as well as calculations on helicene molecules as large scale applications in Sec. IV. In Sec. V some concluding remarks and an outlook on forthcoming work will be given.

II. THEORY

In the following paragraphs, we present the theory for second derivatives of CC2 energies without and with orbital relaxation. All equations presented here for CC2 can be simplified to the respective MP2 expressions by neglecting all contributions from singles cluster amplitudes and singles Lagrangian multipliers (see Eq. (6) as an example for the energy).

A. The CC2 Lagrangian

Using the framework of second quantization and assuming a field-independent atomic orbital basis, we define for the general frequency-dependent case the time-dependent Hamiltonian as[23]

$$\hat{H}(t,x) = \hat{H}^{(0)} + \hat{V}(t,\epsilon). \tag{1}$$

$\hat{H}^{(0)}$ describes here the time-independent unperturbed system and $\hat{V}(t,\epsilon)$ is a time-dependent perturbation of the form

$$\hat{V}(t,\epsilon) = \sum_x \epsilon_x(\omega_x) e^{-i\omega_x t}\hat{h}^x, \tag{2}$$

where ϵ_x are the field strength amplitudes, ω_x frequencies, and $\hat{h}^x$ time-independent operators describing the interaction of the system with the external field. In the following, it is assumed that $\hat{h}^x$ are one-electron operators.

For deriving the equations for second derivatives, we use the well-established Lagrangian technique,[19,24–26] starting with the definition of the Lagrangian for the ground state CC2 energy which in the orbital-unrelaxed case is defined as[6]

$$\begin{aligned} L^{\mathrm{CC2,unrel}} = {} & \langle \mathrm{HF}|\tilde{\hat{H}} + [\tilde{\hat{H}}, \hat{T}_2]|\mathrm{HF}\rangle \\ & + \sum_{\mu_1} \bar{t}_{\mu_1} \langle \mu_1|\tilde{\hat{H}} + [\tilde{\hat{H}}, \hat{T}_2]|\mathrm{HF}\rangle \\ & + \sum_{\mu_2} \bar{t}_{\mu_2} \langle \mu_2|\tilde{\hat{H}} + [\hat{F}^{(0)} + \tilde{\hat{V}}, \hat{T}_2]|\mathrm{HF}\rangle, \end{aligned} \tag{3}$$

Downloaded 21 Sep 2012 to 134.147.252.238. Redistribution subject to AIP license or copyright; see http://jcp.aip.org/about/rights_and_permissions

and for the orbital relaxed case as[26]

$$L^{\mathrm{CC2,rel}} = \langle \mathrm{HF}|\tilde{\hat{H}} + [\tilde{\hat{H}}, \hat{T}_2]|\mathrm{HF}\rangle + \sum_{\mu_1} \bar{t}_{\mu_1} \langle \mu_1|\tilde{\hat{H}} + [\tilde{\hat{H}}, \hat{T}_2]|\mathrm{HF}\rangle + \sum_{\mu_2} \bar{t}_{\mu_2} \langle \mu_2|\tilde{\hat{H}} + [\hat{F}, \hat{T}_2]|\mathrm{HF}\rangle + \sum_{\mu_0} \bar{\kappa}_{\mu_0} F_{\mu_0}. \tag{4}$$

Here and in the following, we denote with $\tilde{\hat{O}}$ similarity-transformed operators defined as $\tilde{\hat{O}} = e^{-\hat{T}_1} \hat{O} e^{\hat{T}_1}$ and with $\hat{T}_1$ and $\hat{T}_2$, respectively, the singles and doubles part of the cluster operator. $\bar{t}_{\mu_1}$ and $\bar{t}_{\mu_2}$ are the Lagrangian multipliers for the singles (μ_1) and doubles (μ_2) excitation manifolds and $\hat{F}^{(0)}$ is the Fock matrix of the unperturbed system, while $\hat{F}$ is the full Fock matrix (including the one-electron perturbation). The last term in Eq. (4) accounts for the equations which determine the orbital rotation parameters κ_{μ_0} and $\bar{\kappa}_{\mu_0}$ are the corresponding Lagrangian multipliers. F_{μ_0} are the Fock matrix elements which are required to vanish. For a closed-shell case, we can express the similarity-transformed Hamiltonian in second quantized form as

$$\tilde{\hat{H}} = \sum_{pq} \tilde{\hat{h}}_{pq} E_{pq} + \frac{1}{2} \sum_{pqrs} (pq|\tilde{rs}) e_{pqrs}, \tag{5}$$

where p, q, r, and s denote both occupied and virtual molecular orbitals and E_{pq} and e_{pqrs} are the usual spin-free one- and two-particle operators.[27] This allows to account for many of the $\hat{T}_1$-dependent contributions by a transformation to a similarity-transformed MO basis.

The Lagrangian for the MP2 energy is obtained as a simplification of Eq. (4) where the contributions from the singles cluster amplitudes and Lagrangian multipliers are omitted:

$$L^{\mathrm{MP2}} = \langle \mathrm{HF}|\hat{H} + [\hat{H}, \hat{T}_2]|\mathrm{HF}\rangle + \sum_{\mu_2} \bar{t}_{\mu_2} \langle \mu_2|\hat{H} + [\hat{F}, \hat{T}_2]|\mathrm{HF}\rangle + \sum_{\mu_0} \bar{\kappa}_{\mu_0} F_{\mu_0}. \tag{6}$$

Within the RI approximation, which is used to increase the efficiency of the method, we expand all correlation contributions to the electron repulsion integrals in an auxiliary basis[20] and express them in terms of three-index intermediates as

$$(pq|rs) \approx (pq|rs)^{RI} = \sum_{Q} B^{Q}_{pq} B^{Q}_{rs} \tag{7}$$

with

$$B^{Q}_{pq} = \sum_{P} (pq|P) V^{-1/2}_{PQ}, \tag{8}$$

$$V_{PQ} = (P|Q), \tag{9}$$

where $(P|Q)$ and $(Q|rs)$ are, respectively, two- and three-index ERIs. Only the Hartree-Fock contributions to the energy and the Fock matrix are (unless otherwise stated) evaluated with the exact four-index ERIs without RI approximation. Using Eq. (7), the CC2 doubles cluster amplitudes can be calculated as[20]

$$t^{ab}_{ij} = -\frac{\sum_Q \hat{B}^{Q}_{ai} \hat{B}^{Q}_{bj}}{\epsilon_a - \epsilon_i + \epsilon_b - \epsilon_j}, \tag{10}$$

where $\hat{B}^{Q}_{ai}$ are three-index intermediates in the similarity-transformed basis. Here and in the following, we use the convention that indices $i, j, \ldots$ refer to occupied orbitals and indices $a, b, \ldots$ to virtual molecular orbitals.

With the above approach the storage of four-index integrals, doubles amplitudes and other quantities of comparable size can be avoided in the calculation of MP2 and CC2 ground state and excitation energies and first-order (transition) properties[19–22] since it becomes affordable to calculate these intermediates on-the-fly from three-index intermediates whenever needed and contract them immediately to low scaling arrays, which can easily be stored in memory or on disc. However, for second- and higher-order properties, additional complications appear in the computation of derivatives of one- and two-particle density matrices (*vide infra*).

B. Derivatives of the Lagrangian

Deriving the Lagrangian in Eq. (4) twice with respect to the strengths of electric fields (referred to as x and y) using the $2n + 1$ and $2n + 2$ rules[24] for, respectively, the response of the cluster amplitudes and Lagrangian multipliers[25,26] results in the expression:

$$\left(\frac{d^2 L^{\mathrm{CC2}}}{dxdy}\right)_{\epsilon=0} = \langle \hat{J}^{xy} \rangle + \mathbf{F} \cdot t^x \cdot t^y + \eta^x \cdot t^y + \eta^y \cdot t^x, \tag{11}$$

with

$$F_{\mu\nu} = \left(\frac{\partial^2 L^{\mathrm{CC2}}}{\partial t_\mu \partial t_\nu}\right)_{\epsilon=0}, \tag{12}$$

$$\eta^x_\mu = \left(\frac{\partial^2 L^{\mathrm{CC2}}}{\partial t_\mu \partial x}\right)_{\epsilon=0} + \sum_{\nu_0} \left(\frac{\partial^2 L^{\mathrm{CC2}}}{\partial t_\mu \partial \kappa_{\nu_0}}\right)_{\epsilon=0} \kappa^x_{\nu_0}, \tag{13}$$

$$\hat{J}^{xy} = \hat{P}^{xy}\left([\hat{\kappa}^x, \hat{h}^y] + \tfrac{1}{2}[\hat{\kappa}^x, [\hat{\kappa}^y, \hat{H}]]\right). \tag{14}$$

In the above equations, we have introduced t^x as short-hand notation for the first derivatives of the cluster amplitudes with respect to a perturbation x while κ^x are the first-derivatives of the orbital rotation parameters. $\langle \hat{J}^{xy} \rangle$ denotes the CC2 or MP2 expectation value of the effective second-order Hamiltonian $\hat{J}^{xy}$ and $\hat{P}^{xy}$ is a symmetrization operator defined by $\hat{P}^{xy} f_{x,y} = f_{x,y} + f_{y,x}$.

For orbital-unrelaxed second-order properties, i.e., second derivatives of the Lagrangian in Eq. (3), the contributions depending on κ^x vanish. In addition there are differences in the first contribution to η^x_μ and in the definition of the right-hand side (RHS) vector for the calculation of the response of the cluster amplitudes. They result from the different treatment of the perturbation in the two cases: In the unrelaxed case, the doubles projection in Eq. (3) contains $[\hat{F}^{(0)} + \tilde{\hat{V}}, \hat{T}_2]$, where $\tilde{\hat{V}}$ includes a similarity transformation with $\hat{T}_1$, while in

Downloaded 21 Sep 2012 to 134.147.252.238. Redistribution subject to AIP license or copyright; see http://jcp.aip.org/about/rights_and_permissions

the relaxed case, the perturbation is included in the Fock matrix, which carries in the contribution $[\hat{F}, \hat{T}_2]$ to the doubles projection no similarity transformation.

C. Response of the amplitudes

The response of the cluster amplitudes is obtained as solution of the linear equations system,[23]

$$\mathbf{A}t^x = \xi^x, \tag{15}$$

where $\mathbf{A}$ is the Jacoby matrix:

$$\mathbf{A}_{\mu\nu} = \left(\frac{\partial^2 L}{\partial \bar{t}_\mu \partial t_\nu}\right)_{\epsilon=0}. \tag{16}$$

Working equations for the CC2 Jacoby matrix have already been reported in Refs. 6, 20 and are not repeated here. We only note that $\mathbf{A}$ is identical in the orbital-relaxed and orbital-unrelaxed cases. The difference between the two ways to take derivatives enters the response equations for the cluster amplitudes only through the RHS vectors:

$$\xi^x_\mu = \left(\frac{\partial^2 L}{\partial \bar{t}_\mu \partial x}\right)_{\epsilon=0} + \sum_{\nu_0}\left(\frac{\partial^2 L}{\partial \bar{t}_\mu \partial \kappa_{\nu_0}}\right)_{\epsilon=0}\kappa^x_{\nu_0}, \tag{17}$$

where the last term is only present in the orbital-relaxed case. For unrelaxed CC2 derivatives, one obtains[23]

$$\xi^{x,\mathrm{unrel}}_{ai} = \sum_{ck}\left(2t^{ac}_{ik} - t^{ac}_{ki}\right)\hat{h}^x_{kc} + \hat{h}^x_{ai}, \tag{18}$$

$$\xi^{x,\mathrm{unrel}}_{aibj} = \hat{P}^{ab}_{ij}\left(\sum_c t^{ac}_{ij}\hat{h}^x_{cb} - \sum_k t^{ab}_{ik}\hat{h}^x_{kj}\right), \tag{19}$$

where $\hat{h}^x$ denotes the first derivative of the one-electron integrals and $\hat{P}^{pr}_{qs}$ is a symmetrization operator defined by $\hat{P}^{pr}_{qs} f_{pq,rs} = f_{pq,rs} + f_{rs,pq}$. In the orbital-relaxed case, the singles and doubles parts of ξ^x are—within the RI approximation—given by

$$\begin{aligned}\xi^{x,\mathrm{rel}}_{ai} = {} & \sum_{ck}\left(2t^{ac}_{ik} - t^{ac}_{ki}\right)\hat{F}_{kc}[\hat{J}^x] + \hat{F}_{ai}[\hat{J}^x] \\ & + \sum_{cdk}\left(2t^{cd}_{ik} - t^{cd}_{ki}\right)\hat{P}^{ka}_{dc}\left(\sum_Q \hat{B}^Q_{kd}[\hat{J}^x]\hat{B}^Q_{ac}\right) \\ & + \sum_{dkl}\left(2t^{ad}_{kl} - t^{ad}_{lk}\right)\hat{P}^{lk}_{di}\left(\sum_Q \hat{B}^Q_{ld}[\hat{J}^x]\hat{B}^Q_{ki}\right),\end{aligned} \tag{20}$$

$$\begin{aligned}\xi^{x,\mathrm{rel}}_{aibj} = {} & \hat{P}^{ab}_{ij}\left(\sum_c t^{ac}_{ij}F_{cb}[\hat{J}^x] - \sum_k t^{ab}_{ik}F_{kj}[\hat{J}^x]\right. \\ & \left. + \sum_Q \hat{B}^Q_{ai}[\hat{J}^x]\hat{B}^Q_{bj}\right).\end{aligned} \tag{21}$$

With $F^x[\hat{J}^x]_{pq}$ and $B^Q_{pq}[\hat{J}^x]$, we denote, respectively, the MO Fock matrix and the three-index ERIs computed from the integrals for the effective first-order Hamiltonian

$$\hat{J}^x = \hat{h}^x + [\hat{\kappa}^x, \hat{H}], \tag{22}$$

instead of those for $\hat{H}$. The explicit expressions are

$$\begin{aligned}F_{pq}[\hat{J}^x] = {} & h^x_{pq} + (\epsilon_q - \epsilon_p)\kappa^x_{pq} \\ & + \sum_{rs}\kappa^x_{sr}(\nu_s - \nu_r)\left((pq|rs) - \tfrac{1}{2}(ps|rq)\right),\end{aligned} \tag{23}$$

$$B^Q_{pq}[\hat{J}^x] = \sum_t\left(\kappa^x_{pt}B^Q_{tq} - B^Q_{pt}\kappa^x_{tq}\right), \tag{24}$$

where ν_p are the SCF orbital occupation numbers (0 or 2). Note that after the solution of the CPHF equations for κ^x, the virtual/occupied elements of $F_{pq}[\hat{J}^x]$ in Eq. (23) vanish. $\hat{F}[\hat{J}^x]$ and $\hat{B}^Q[\hat{J}^x]$ are the similarity-transformed counterparts computed from the integrals for $\exp(-\hat{T}_1)\hat{J}^x\exp(\hat{T}_1)$. For consistency with the way the unperturbed Fock matrix $\hat{F}_{pq}$ is evaluated in the ground state cluster equations, the t_1-dependent correlation contributions to $\hat{F}[\hat{J}^x]$, which are not part of $F_{pq}[\hat{J}^x]$, are evaluated within the RI approximation:

$$\begin{aligned}\hat{F}_{pq}[\hat{J}^x] = {} & F_{pq}[\hat{J}^x] + \sum_r(F_{pr}[\hat{J}^x]t_{rq} - t_{pr}F_{rq}[\hat{J}^x]) \\ & + \sum_{ck,Q} t_{ck}\hat{P}^{pk}_{qc}\left(2\hat{B}^Q_{pq}[\hat{J}^x]\hat{B}^Q_{kc} - \hat{B}^Q_{kq}[\hat{J}^x]\hat{B}^Q_{pc}\right).\end{aligned} \tag{25}$$

For the ease of notation, we have in the second term of Eq. (25) extended t_1 to a matrix in the full MO space with the understanding that all other than the virtual/occupied elements are zero.

Since for CC2 the doubles–doubles block of the Jacobian is diagonal in the canonical MO basis, the response equations (15) can be reduced to an effective linear equation system within only the singles subspace:[20]

$$\mathbf{A}^{\mathrm{eff}}_{SS}t^x_S = \xi^{x,\mathrm{eff}}_S, \tag{26}$$

$$\mathbf{A}^{\mathrm{eff}}_{SS} = \mathbf{A}_{SS} - \frac{\mathbf{A}_{SD}\mathbf{A}_{DS}}{\mathbf{A}_{DD} - \omega\mathbf{1}}, \tag{27}$$

where S and D denote the singles and doubles blocks of the Jacobian matrix and the RHS and solution vectors. Explicit expressions for the CC2 effective Jacobian were reported in Ref. 6. Following the approach outlined in Refs. 20 and 21, we obtain for the corresponding effective singles RHS vector:

$$\xi^{x,\mathrm{eff}}_S = \xi^x_S - \mathbf{A}_{SD}\left(\mathbf{A}_{DD} - \omega\mathbf{1}\right)^{-1}\xi^x_D. \tag{28}$$

After solution of the equations for t^x_{ai}, the response of the doubles amplitudes is obtained from the non-iterative expression

$$t^{ab,x}_{ij} = -\frac{\xi^x_{aibj} + \sum_Q \hat{P}^{ab}_{ij}\bar{B}^{x,Q}_{ai}\hat{B}^Q_{bj}}{\epsilon_a - \epsilon_i + \epsilon_b - \epsilon_j}, \tag{29}$$

where the intermediates $\bar{B}^{x,Q}_{ai}$ are similarity transformed with the response of the singles amplitudes according to

$$\bar{B}^{x,Q}_{ai} = \sum_c t^x_{ci}\hat{B}^Q_{ac} - \sum_k t^x_{ak}\hat{B}^Q_{ki}. \tag{30}$$

Similar as the other double excitation intermediates, also $t^{ab,x}_{ij}$ is never stored in our RI-CC2 implementation. Instead, it is

Downloaded 21 Sep 2012 to 134.147.252.238. Redistribution subject to AIP license or copyright; see http://jcp.aip.org/about/rights_and_permissions

calculated on-the-fly from two- and three-index intermediates and contracted immediately with other integral intermediates or Lagrangian multipliers to quantities which can easily be stored in memory or on disc. For MP2, t_{ai}^{x} and $\xi_{ai}^{x,\mathrm{eff}}$ vanish since the singles amplitudes are zero and $t_{ij}^{ab,x}$ simplifies to

$$t_{ij}^{ab,x} = -\frac{\sum_Q \hat{P}_{ij}^{ab}\left(B_{ai}^{Q}[\hat{J}^x]B_{bj}^{Q}\right)}{\epsilon_a - \epsilon_i + \epsilon_b - \epsilon_j}. \tag{31}$$

D. First-order densities and effective Fock matrices

The evaluation of the dot products $\eta^x \cdot t^y$ from Eq. (11) as such is not well suited for an RI-CC2 implementation where one wants to avoid the storage of double excitation intermediates. The simultaneous on-the-fly construction of the double excitation parts of η^x and t^y for all relevant pairs of perturbations can lead to large core memory requirements and a complicated book keeping and would have a high prefactor for the $\mathcal{O}(\mathcal{N}^5)$-scaling steps. To avoid this problem, we rewrite these dot products as contractions of first-order densities, depending on t^y, with the integrals for $\hat{h}^x$ in the unrelaxed case,

$$\eta^{x,\mathrm{unrel}} \cdot t^y = \sum_{pq} D_{pq}^{\eta}(t^x)\hat{h}_{pq}^{x}, \tag{32}$$

and with Fock matrices and three-index integral-intermediates for the effective first-order Hamiltonian $\hat{J}^x$ in the relaxed case:

$$\eta^{x,\mathrm{rel}} \cdot t^y = \sum_{pq} D_{pq}^{F,\eta}(t^y)F_{pq}[\hat{J}^x] + \frac{1}{2}\sum_{pqrs} \hat{d}_{pqrs}^{\mathrm{nsep},\eta}(t^y)\hat{P}_{qs}^{pr}\left(\sum_Q \hat{B}_{pq}^{Q}[\hat{J}^x]\hat{B}_{rs}^{Q}\right). \tag{33}$$

Note that the one-electron density $D_{pq}^{\eta}(t^x)$ in Eq. (32) and the two-electron density $\hat{d}_{pqrs}^{\mathrm{nsep},\eta}(t^x)$ in Eq. (33) are contracted with integrals in the t_1-dependent similarity-transformed MO basis, while $D_{pq}^{F,\eta}(t^x)$ refers to the unmodified MO basis. Explicit expressions for D_{pq}^{η} have been reported in Ref. 21. The one- and two-electron densities $D_{pq}^{F,\eta}$ and $\hat{d}_{pqrs}^{\mathrm{nsep},\eta}$, needed in the orbital-relaxed case, are defined as

$$\begin{aligned} D_{pq}^{F,\eta}(t^x) = {} & \langle \mathrm{HF}|\left[E_{pq}, \hat{T}_1^x\right]|\mathrm{HF}\rangle \\ & + \sum_{\mu_1} \bar{t}_{\mu_1}^{(0)}\langle \mu_1|\left[E_{pq}, \hat{T}_1^x\right] + \left[\left[E_{pq}, \hat{T}_1^{(0)}\right], \hat{T}_1^x\right] \\ & + \left[E_{pq}, \hat{T}_2^x\right]|\mathrm{HF}\rangle + \sum_{\mu_2} \bar{t}_{\mu_2}^{(0)}\langle \mu_2|\left[E_{pq}, \hat{T}_2^x\right]|\mathrm{HF}\rangle, \end{aligned} \tag{34}$$

$$\begin{aligned} \hat{d}_{pqrs}^{\mathrm{nsep},\eta}(t^x) = {} & \langle \mathrm{HF}|\left[[e_{pqrs}, \hat{T}_1], \hat{T}_1^x\right] + \left[e_{pqrs}, \hat{T}_2^x\right]|\mathrm{HF}\rangle \\ & + \sum_{\mu_1} \bar{t}_{\mu_1}^{(0)}\langle \mu_1|\left[e_{pqrs}, \hat{T}_1^x\right] + \left[\left[e_{pqrs}, \hat{T}_1^x\right], \hat{T}_2\right] \\ & + \left[e_{pqrs}, \hat{T}_2^x\right]|\mathrm{HF}\rangle + \sum_{\mu_2} \bar{t}_{\mu_2}^{(2)}\langle \mu_2|\left[e_{pqrs}, \hat{T}_1^x\right]|\mathrm{HF}\rangle. \end{aligned} \tag{35}$$

TABLE I. Expressions for the one-particle density $D^{F,\eta}$. The expressions for $D_{ab}^{F,\eta}$ and $D_{ij}^{F,\eta}$ are the same as those given for the unrelaxed case in Ref. 21.

$D_{ij}^{F,\eta}(t^x) = -\sum_a \bar{t}_{aj}t_{ai}^{x} - \sum_{abk} \bar{t}_{jk}^{ab}t_{ik}^{x,ab}$
$D_{ab}^{F,\eta}(t^x) = \sum_i \bar{t}_{ai}t_{bi}^{x} + \sum_{cij} \bar{t}_{ij}^{ac}t_{ij}^{x,bc}$
$D_{ia}^{F,\eta}(t^x) = 2t_{ai}^{x} - \sum_{ck} \bar{t}_{ck}(t_{ak}t_{ci}^{x} + t_{ak}^{x}t_{ci}) - \sum_{bj}(2t_{ij}^{ab,x} - t_{ji}^{ab,x})\bar{t}_{bj}$
$D_{ai}^{F,\eta}(t^x) = 0$

$D^{F,\eta}$ and $\hat{d}^{\mathrm{nsep},\eta}$ are closely related to the densities D^A and d^A which have been described in the formation of the excited state gradient.[22] They just differ in a contribution which results from the differentiation of the CC2 energy expression which is not taken into account in D^A and d^A. Explicit expressions for $D^{F,\eta}$ are given in Table I, and expressions for $\hat{d}^{\mathrm{nsep},\eta}$ are given in the supplementary material.[28]

The last part of Eq. (33) is rewritten as a contraction of a a three-index density $\Delta_{pq}^{\eta,Q,x}$ with three-index integrals:

$$\sum_{pqrs} \hat{d}_{pqrs}^{\mathrm{nsep},\eta}(t^x)\hat{P}_{rs}^{pq}\sum_Q\left(\hat{B}_{pq}^{Q}[\hat{J}^y]\hat{B}_{rs}^{Q}\right) = 2\sum_{pqQ}\Delta_{pq}^{\eta,Q,x}(t^x)\hat{B}_{pq}^{Q}[\hat{J}^y]. \tag{36}$$

In the last equation, we have used the particle exchange symmetry between the index pairs pq and rs. The expression on the right hand side of (36) has the advantage that is does not require any storage of intermediates with $\mathcal{N}^4$-scaling size. For the present case, where $\hat{B}_{pq}^{Q}[\hat{J}^y]$ can be written as one-index transformation of unperturbed ERIs with κ^y, we rewrite this contribution further in terms of so-called "effective Fock matrices" $F^{\mathrm{eff},x,\eta}$ depending only on one perturbation, while the other perturbation is taken into account by contraction with κ^y.

$$\sum_{pqQ}\Delta_{pq}^{\eta,Q,x}\hat{B}_{pq}^{Q}[\hat{J}^y] = \sum_{pt}\kappa_{pt}^{y}F_{pt}^{\mathrm{eff},x,\eta}. \tag{37}$$

Thereby we can avoid the calculation of costly intermediates which depend on two perturbations. Explicit expressions for $F_{pt}^{\mathrm{eff},x,\eta}$ are given in the supplementary material.[28] We only note here that the most important and time-consuming step in the calculation of $\Delta_{pq}^{\eta,Q,x}$ and $F_{pt}^{\mathrm{eff},x,\eta}$ is the formation of intermediates obtained by contracting $\bar{t}_{ij}^{ab}$, t_{ij}^{ab}, and $t_{ij}^{ab,x}$ with different three-index integrals. These contractions are done simultaneously with the computation of the one-electron densities $D^{F,\eta}$.

E. The expectation value of $\hat{J}^{xy}$

To evaluate the expectation value of the effective second-order Hamiltonian $\hat{J}^{xy}$, we use that

$$\langle (S, \hat{O})\rangle = \sum_{pq} F_{pq}^{\mathrm{eff}}[\hat{O}]S_{pq}, \tag{38}$$

where $(S, \hat{O})$ denotes a one-index transformation of the integral for the operator $\hat{O}$ with S as transformation matrix.

Downloaded 21 Sep 2012 to 134.147.252.238. Redistribution subject to AIP license or copyright; see http://jcp.aip.org/about/rights_and_permissions

For a real antisymmetric orbital-rotation matrix κ_{pq}, we have $[\hat{\kappa}, \hat{O}] = (\kappa, \hat{O})$. To apply Eq. (38), we write $\hat{J}^{xy}$ as a sum of two one-index transformed first-order operators

$$\hat{J}^{xy} = [\hat{\kappa}^x, \hat{\mathcal{J}}^y] + [\hat{\kappa}^y, \hat{\mathcal{J}}^x], \tag{39}$$

with

$$\hat{\mathcal{J}}^x = \hat{h}^x + \tfrac{1}{2}[\hat{\kappa}^x, \hat{H}]. \tag{40}$$

Note that $\hat{\mathcal{J}}^x$ differs from $\hat{J}^x$ defined in Eq. (22) by a factor of $\frac{1}{2}$ in front of the second term. We thus compute the expectation value of $\hat{J}^{xy}$ as

$$\langle \hat{J}^{xy} \rangle = \sum_{pq} \kappa^x_{pq} F^{\text{eff},y}_{pq} + \sum_{pq} \kappa^y_{pq} F^{\text{eff},x}_{pq}, \tag{41}$$

where $F^{\text{eff},y}$ denotes the effective Fock matrix obtained with integrals for $\hat{\mathcal{J}}^x$. It can be computed similar to F^{eff} for the unperturbed Hamiltonian, which is used in the calculation of gradients,[19] as

$$\begin{aligned} F^{\text{eff},y}_{pq} = &\sum_t \left(D^{\text{eff}}_{pt} F_{qt}[\hat{\mathcal{J}}^y] + D^{\text{eff}}_{tp} F_{tq}[\hat{\mathcal{J}}^y] \right) \\ &+ \frac{\nu_p}{4} \left(G\{D^{\text{corr}}\}^{\kappa_y}_{qp} + G\{D^{\text{corr}}\}^{\kappa_y}_{pq} \right) \\ &+ \sum_{Qt} \left(\Delta^Q_{pt} B^Q_{qt}[\hat{\mathcal{J}}^y] + \Delta^{Q,y}_{pt} B^Q_{qt} + \Delta^Q_{tp} B^Q_{tq}[\hat{\mathcal{J}}^y] \right. \\ &\left. + \Delta^{Q,y}_{tp} B^Q_{tq} \right), \end{aligned} \tag{42}$$

where $G\{D^{\text{corr}}\}^{\kappa^y}_{pq}$ is defined as

$$\begin{aligned} G\{D^{\text{corr}}\}^{\kappa^y}_{pq} = &\sum_t \left(\kappa^y_{pt} \sum_{rs} D^{\text{corr}}_{rs} A_{tqrs} + \kappa^y_{tq} \sum_{rs} D^{\text{corr}}_{rs} A_{ptrs} \right) \\ &+ \sum_{rst} \left(D^{\text{corr}}_{ts} \kappa^y_{tr} + \kappa^y_{ts} D^{\text{corr}}_{rt} \right) A_{pqrs}. \end{aligned} \tag{43}$$

In these equations, D^{eff} is the relaxed one-particle density and $D^{\text{corr}} = D^{\text{eff}} - D^{\text{SCF}}$, the matrix A_{pqrs} is defined as $A_{pqrs} = 4(pq|rs) - (pr|sq) - (ps|rq)$, and ν_p are again the SCF occupation numbers. Detailed working expressions are given in the supplementary material.[28] The implementation of $F^{\text{eff},y}$ uses essentially the same techniques as described in Ref. 19 for the matrix F^{eff}, which is used to compute the RI-CC2 ground state gradients.

F. Contraction with the cluster amplitude Hessian F

For the last contribution, we have to contract the matrix of second derivatives of the Lagrangian with respect to cluster amplitudes, **F**, with two first-order amplitude vectors. Non-vanishing contributions are obtained from the contraction with either two singles vectors or one singles and one doubles vector, while the contribution from two doubles vectors vanishes due to the structure of the CC2 cluster equations:

TABLE II. Intermediates needed for the contraction of the matrix **F** with the response of the amplitudes. $(pq\bar{|}rs)$ denote two-electron integrals transformed with the response of the singles cluster amplitudes. All ERIs are calculated within the RI approximation.

$\sigma^{0,x}_{ai} = \sum_{ck} [2(ia\hat{\|}kc) - (ic\|ka)] t^x_{ck}$
$\sigma^{F,x}_{ai} = \sum_{cdk} \bar{t}^{cd}_{ki} (ck\hat{\|}da)^x - \sum_{ckl} \bar{t}^{ca}_{kl} (ck\hat{\|}il)$
$\sigma^{G,x}_{ai} = -\sum_j \bar{t}_{aj} \sum_{cdk} t^{cd,x}_{jk} [2(kd\|ic) - (kc\|id)]$
$\sigma^{H,x}_{ai} = \sum_b \bar{t}_{bi} \sum_{dkl} t^{bd,x}_{kl} [2(ld\|ka) - (la\|kd)]$
$\sigma^{I,x}_{ai} = \sum_{bj} \bar{t}_{bj} \sum_{ck} \left[2t^{bc,x}_{jk} - t^{cb,x}_{jk} \right] \left[2(kc\|ia) - (ic\|ka) \right]$
$\sigma^{J,x}_{ai} = \sum_b \bar{t}_{bi} \bar{F}^x_{ba} - \sum_j \bar{t}_{aj} \bar{F}^x_{ij} + \sum_{bj} \bar{t}_{bj} \left[2(bj\bar{\|}ia) - (ij\bar{\|}ba) \right]$
$\bar{F}^x_{ia} = \sum_{ck} [2(ia\|kc) - (ic\|ka)] t^x_{ck}$
$\bar{F}^x_{ab} = -\sum_j t^x_{aj} \hat{F}_{jb} + \sum_{ck} [2(ab\|kc) - (ac\|kb)] t^x_{ck}$
$\bar{F}^x_{ij} = \sum_b \hat{F}_{jb} t^x_{bi} + \sum_{ck} [2(ij\|kc) - (ic\|kj)] t^x_{ck}$

$$\begin{aligned} \sum_{\mu\nu} \mathbf{F}_{\mu\nu} t^x_\mu t^y_\nu = &\sum_{\mu_1\nu_1} \langle \text{HF} | \left[\left[\tilde{\hat{H}}, \tau_{\mu_1} \right], \tau_{\nu_1} \right] | \text{HF} \rangle t^x_{\mu_1} t^y_{\nu_1} \\ &+ \sum_{i=1,2} \sum_{\lambda_i \mu_1 \nu_1} \bar{t}_{\lambda_i} \langle \lambda_i | \left[\left[\tilde{\hat{H}}, \tau_{\mu_1} \right], \tau_{\nu_1} \right] | \text{HF} \rangle t^x_{\mu_1} t^y_{\nu_1} \\ &+ \hat{P}^{xy} \sum_{\lambda_1 \mu_1 \nu_2} \bar{t}_{\lambda_1} \langle \lambda_1 | \left[\left[\tilde{\hat{H}}, \tau_{\mu_1} \right], \tau_{\nu_2} \right] | \text{HF} \rangle t^x_{\mu_1} t^y_{\nu_2}. \end{aligned} \tag{44}$$

This allows to rewrite all contributions as contraction of singles amplitudes vectors with another one-electron intermediate:

$$\begin{aligned} \sum_{\mu\nu} \mathbf{F}_{\mu\nu} t^x_\mu t^y_\nu = &\sum_{ai} \sigma^{0,x}_{ai} t^y_{ai} + \sum_{ai} \sigma^{F,x}_{ai} t^y_{ai} + \sum_{ai} \sigma^{G,x}_{ai} t^y_{ai} \\ &+ \sum_{ai} \sigma^{G,y}_{ai} t^x_{ai} + \sum_{ai} \sigma^{H,x}_{ai} t^y_{ai} - \sum_{ai} \sigma^{H,y}_{ai} t^x_{ai} \\ &+ \sum_{ai} \sigma^{I,x}_{ai} t^y_{ai} + \sum_{ai} \sigma^{I,y}_{ai} t^x_{ai} + \sum_{ai} \sigma^{J,x}_{ai} t^y_{ai}. \end{aligned} \tag{45}$$

Explicit expressions for the contributions are given in Table II. The contractions $\mathbf{F} \cdot t^x \cdot t^y$ can thus be evaluated with an operation count $\propto n_{\text{pert}} O^2 V^2 N_X$, where O, V, and N_X are, respectively, the number of occupied, virtual, and auxiliary basis functions and n_{pert} is the number of perturbations. The storage demands scale in our implementation as $\mathcal{O}(n_{\text{pert}} O V N_X)$.

Since all contributions from the cluster amplitude Hessian **F** are at least linear in the response of the singles amplitudes, they vanish for MP2.

III. IMPLEMENTATION

The approach described above has been implemented in a development version of the ricc2 program of the TURBOMOLE (Ref. 29) package. All through the implementation storage of $\mathcal{O}(\mathcal{N})^4$-scaling intermediates is avoided to reduce the disc

Downloaded 21 Sep 2012 to 134.147.252.238. Redistribution subject to AIP license or copyright; see http://jcp.aip.org/about/rights_and_permissions

space demands. The unperturbed cluster amplitudes are calculated as described in Ref. 20 and the Lagrangian multipliers $\bar{t}$ as described in Ref. 21. The calculation of the response of the orbital rotation parameters κ^x uses the same techniques which are also used for $\bar{\kappa}$.

A. The effective right-hand-side vector ξ^{eff}

The algorithm for constructing the effective right-hand-side vectors for the first-order response equations, ξ^{eff}, is shown in Fig. 1. Storage of N^4-scaling arrays is avoided by calculating the unperturbed doubles amplitudes twice—once in a loop over occupied orbitals for the contraction with the virtual-virtual block of the perturbed one-electron integrals and a second time in a loop over virtual orbitals for the contraction with the occupied-occupied block of the one-electron integrals. Due to the on-the-fly generation of the doubles amplitudes, the three-index intermediates $\hat{B}^Q_{ai}$ have to be resorted such that for the first loop the occupied and for the second loop the virtual index is outermost (see Fig. 1). Also the contributions to the $\bar{Y}$ intermediates obtained in this second step are after completion resorted such that the occupied index is running outermost, which is the order used in the subsequent routines. The solution of the response equations follows the framework presented in Ref. 21.

- loop I (subset of occupied orbitals i)
  - read $\hat{B}^Q_{ai}$ for $i \in I$
  - loop J (subset of occupied orbitals j)
    - read $\hat{B}^Q_{bj}$, B^Q_{jb} for $j \in J$
    - $t^{ab}_{ij} = -\left(2\hat{B}^Q_{ai}\hat{B}^Q_{bj} - \hat{B}^Q_{aj}\hat{B}^Q_{bi}\right)(\epsilon_a - \epsilon_i + \epsilon_b - \epsilon_j)^{-1}$
    - $\hat{\xi}^{x,ab}_{ij} = t^{ac}_{ij}\hat{h}^x_{bc} + t^{cb}_{ij}\hat{h}^x_{ac}$ and $\xi^{x,\text{eff}}_{ai} += t^{ab}_{ij}\hat{h}^x_{bj}$
    - $\bar{Y}^Q_{ai} += \hat{\xi}^{x,ab}_{ij}B^Q_{jb}$
  - end loop J
  - store $\bar{Y}^Q_{ai}$ on disc
- end loop I
- resort $\hat{B}^Q_{ai}$ and B^Q_{ia} such that the leading index is virtual
- loop A (subset of virtual orbitals a)
  - read $\hat{B}^Q_{ai}$ for $a \in A$
  - loop B (subset of virtual orbitals b)
    - read $\hat{B}^Q_{bj}$, B^Q_{jb} for $b \in B$
    - $t^{ab}_{ij} = -\left(2\hat{B}^Q_{ai}\hat{B}^Q_{bj} - \hat{B}^Q_{aj}\hat{B}^Q_{bi}\right)(\epsilon_a - \epsilon_i + \epsilon_b - \epsilon_j)^{-1}$
    - $\hat{\xi}^{x,ab}_{ij} = -t^{ab}_{ik}\hat{h}^x_{jk} - t^{ab}_{kj}\hat{h}^x_{ki}$
    - $\bar{Y}^Q_{ai} += \hat{\xi}^{x,ab}_{ij}B^Q_{jb}$
  - end loop B
  - store $\bar{Y}^Q_{ai}$ on disc
- end loop A

FIG. 1. Scheme for time-determining steps in the construction of the RHS vectors ξ^x.

B. First-order one-particle densities

As can be seen from the definitions in Table I and Ref. 21, the calculation of the densities $D^{F,\eta}$ and D^{η} requires a contraction of $t^{ab,x}_{ij}$ (Eq. (29)) with the ground state doubles Lagrangian multipliers $\bar{t}^{ab}_{ij}$ over two virtual and one occupied index for the occ./occ. block and over two occupied and one virtual index for the vir./vir. block. Since $t^{ab,x}_{ij}$ depends on the unperturbed doubles amplitudes t^{ab}_{ij} (Eq. (10)), we end up with an expression depending on three different four-index intermediates with three different sets of indices which can only be handled efficiently if at least one of them is either stored as four-index quantity or decomposed to a lower rank intermediate. We pursue the latter option and apply for the decomposition of a numerical Laplace transformation of the orbital energy denominator in Eq. (10)):

$$\frac{1}{\epsilon_a - \epsilon_i + \epsilon_b - \epsilon_j} = \int_0^\infty e^{-(\epsilon_a-\epsilon_i+\epsilon_b-\epsilon_j)\theta}d\theta \tag{46}$$

$$\approx \sum_m^{N_m} \omega_m e^{-(\epsilon_a-\epsilon_i)\theta_m}e^{-(\epsilon_b-\epsilon_j)\theta_m}. \tag{47}$$

N_m is the number of Laplace sampling points, θ_m are the sampling points themselves, and ω_m are the weights. The exponential factors and weights are combined with the three-index integrals $\hat{B}^Q_{ai}$ to intermediates $\hat{K}^{Q,m}_{ai}$,

$$\hat{K}^{Q,m}_{ai} = \hat{B}^Q_{ai}\sqrt{\omega_m}e^{-(\epsilon_a-\epsilon_i)\theta_m}. \tag{48}$$

With these we can approximate the doubles amplitudes as[30]

$$t^{ab}_{ij} \approx -\sum_{Q,m}\hat{K}^{Q,m}_{ai}\hat{K}^{Q,m}_{bj}, \tag{49}$$

and rewrite the RHS vector for the orbital-relaxed first-order amplitudes ξ^x_{aibj}, Eq. (21), as

$$\xi^{x,\text{rel}}_{aibj} = \hat{P}^{ab}_{ij}\left(\sum_{mQ}\hat{K}^{Q,m}_{ai}\bar{K}^{Q,m,x}_{bj} + \sum_Q \hat{B}^Q_{ai}[\hat{J}^x]\hat{B}^Q_{bj}\right) \tag{50}$$

with

$$\bar{K}^{Q,m,x}_{ai} = \sum_c \hat{K}^{Q,m}_{ci}F_{ac}[\hat{J}^x] - \sum_k \hat{K}^{Q,m}_{ak}F_{ki}[\hat{J}^x]. \tag{51}$$

The one-index transformation with the perturbed Fock matrix has thereby been absorbed into $\bar{K}^{Q,m,x}$ and the contractions of doubles Lagrangian multipliers with responses of the doubles amplitudes can be evaluated without storing a four-index quantity. The same approach is also used in the unrelaxed case (compare Eq. (19)) for the contribution from $[\tilde{\hat{V}}, \hat{T}_2]$ to $t^{ab,x}_{ij}$.

Equation (50) requires that four-index integral-type intermediates are formed not only twice as in Eq. (21) but $N_m + 1$ times if N_m is the number of sampling points. Since the formation of these intermediates is the most time-consuming step in RI-CC2 calculations in general, the calculation time depends significantly on the number of Laplace sampling points. As will be demonstrated later, the error caused by the numerical Laplace transformation in this step is very small even for a small number of sampling points. The algorithm for the time-

Downloaded 21 Sep 2012 to 134.147.252.238. Redistribution subject to AIP license or copyright; see http://jcp.aip.org/about/rights_and_permissions

- construct $\hat{K}^{Q,m}_{ai}$, $\bar{K}^{Q,m,x}_{ai}$, $\bar{B}^{Q}_{ai}$
- loop i, j
  - $(b\bar{i}|cj) = \hat{P}^{bc}_{ij}\bar{B}^{Q}_{bi}\hat{B}^{Q}_{cj}$
  - $(b\bar{i}|cj)+ = \hat{P}^{bc}_{ij}\bar{K}^{Q,m,x}_{bi}\hat{K}^{Q,m}_{cj}$
  - $t^{bc,x}_{ij} = -(b\bar{i}|cj)(\epsilon_b - \epsilon_i + \epsilon_c - \epsilon_j)^{-1}$
  - $\bar{t}^{ac}_{ij} = \left(2(a\breve{i}|cj) - (aj|\breve{cj})\right)(\epsilon_i - \epsilon_a + \epsilon_j - \epsilon_c)^{-1}$
  - $D^{\eta}_{ab}+ = \bar{t}^{ac}_{ij}t^{bc,x}_{ij}$
  - $\bar{D}^{\eta}_{ai}- = \left(2t^{ab,x}_{ij} - t^{ab,x}_{ji}\right)\bar{t}_{bj}$
- end loop i ,j

FIG. 2. Algorithm for the computation of the doubles contributions to the virtual/virtual and occupied/virtual block of the one-particle density $D^{\eta}(t^x)$ with a Laplace transformation for $t^{bc,x}_{ij}$. The doubles contribution $\sum_{abk}\bar{t}^{ab}_{jk}t^{ab,x}_{ik}$ to the occupied/occupied block is evaluated in a similar loop over virtual orbitals a, b. For this, the intermediates B and K are resorted such that the virtual index is outermost.

determining steps in the computation of D^{η} with the Laplace transformation is sketched in Fig. 2.

If the orbital relaxation is included, the Laplace transformation can be circumvented if the derivative of the Fock matrix $F[\hat{J}^x]$ can be kept diagonal following the lines of Ref. 31. In this case, $\xi^{x,\mathrm{rel}}_{aibj}$ reduces to

$$\xi^{x,\mathrm{rel}}_{aibj} = P^{ab}_{ij}\left(t^{ab}_{ij}\epsilon^x_b - t^{ab}_{ij}\epsilon^x_j + \sum_Q \hat{B}^Q_{ai}[\hat{J}^x]\hat{B}^Q_{bj}\right), \qquad (52)$$

where ϵ^x_p are the first derivatives of the orbital energies ϵ_p. Similar as the reformulation in Eq. (50), this removes one summation compared to Eq. (21), but without increasing the number of $\mathcal{O}(O^2VN_X)$-scaling steps since the summation is removed by keeping $F[\hat{J}^x]$ (Eq. (23)) diagonal. This degree of freedom can, however, only be used in the orbital-relaxed case and if there is no degeneracy or near-degeneracy between orbitals of the same symmetry.

IV. APPLICATIONS

A. Computational efficiency and large scale application

The RI approximation is known to give large computational savings in MP2 and CC2 calculations of ground state and excitation energies, gradients, first-order properties, and transition moments. In Table III, we listed some selected wall-clock timings for static polarizabilities of medium-sized molecules with and without symmetry computed with unrelaxed CC2 and with orbital-relaxed MP2. We note that orbital-relaxed CC2 offers no improvement for polarizabilities compared to orbital-relaxed MP2 but always results in longer calculation times. Unrelaxed CC2, however, can, in difference to MP2, also be applied to frequency-dependent polarizabilities. Orbital-relaxed CC2 is therefore in the following not taken into account.

The results in Table III show that relatively large molecules can be treated in reasonably short time. Even without symmetry an unrelaxed CC2 calculation of the whole dipole polarizability tensor for naphthacene ($C_{18}H_{12}$, 1104 basis functions) takes only slightly longer than 5 days if run sequentially on a Xeon E5345 central processing unit (CPU) with 2.33 GHz. Using an OpenMP parallelization on 12 cores of two Xeon X5670 (2.93 GHz) CPUs and exploiting D_{2h} point group symmetry, the dipole polarizability of C_{60} can be computed at the MP2 level within less than 10 h.

TABLE III. Wall-clock timings for several aromatic hydrocarbons and C_{60}. In all calculations except for C_{60}, the full tensor was computed using the aug-cc-pVTZ basis[32,33] with the corresponding auxiliary basis[34] and the frozen core for approximation for the 1*s* orbitals of the carbon atoms. N_m is the number of sampling points for the numerical Laplace transformation.

			No. of functions			No.	
Molecule	Method	Sym.	Basis	aux. basis	N_m	Threads	(min) CPU
C_6H_6	CC2, unrel.	D_{2h}	414	912	4	1	13 …[a]
C_6H_6	MP2, rel.	D_{2h}	414	912	4	1	15 …[a]
$C_{10}H_8$	CC2, unrel.	C_1	644	1428	4	1	171 …[b]
$C_{10}H_8$	CC2, unrel.	D_{2h}	644	1428	4	1	49 …[b]
$C_{10}H_8$	MP2, rel.	D_{2h}	644	1428	[c]	1	59 …[a]
$C_{18}H_{12}$	CC2, unrel.	C_1	1104	2460	4	1	7381 …[b]
$C_{18}H_{12}$	CC2, unrel.	D_{2h}	1104	2460	4	1	316 …[a]
$C_{18}H_{12}$	MP2, rel.	D_{2h}	1104	2460	4	1	503 …[a]
C_{60}	CC2, unrel.	D_{2h}	2760	6360	3	1	5493 …[b]
C_{60}	MP2, rel.	D_{2h}	2760	6360	6	12	582 …[d]

[a]Intel(R) Xeon(R) E 5345, 2.33 GHz.
[b]Intel(R) Xeon(R) E 5345, 2.66 GHz.
[c]Calculation done without Laplace algorithm using a canonical $F[\hat{J}^x]$ (Eq. (52)).
[d]Intel(R) Xeon(R) X5670, 2.93 GHz.

To study the behavior of the OpenMP parallelization in more detail, we carried out a series of calculations with unrelaxed CC2 on C_{60} and some aromatic hydrocarbons. The results are shown in Fig. 3. The corresponding data are tabulated in the supplementary material.[28] In particular for the calculations on C_{60} and on naphthalene and naphthacene without symmetry, we obtain good speedups. As can be seen from Fig. 3, the slope of the speedup for naphthacene with C_1-symmetry shows nearly no change between one and four CPUs. For naphthacene and C_{60}, the efficiency is above 90% between one and two CPUs and about 85% between one and four CPUs. For the calculations on naphthalene and naphthacene with D_{2h}-symmetry, the problem size is to small to achieve a good work load balance on more than 4 CPUs and the parallelization becomes then inefficient. Apart from symmetry, the load balance and the speedup depends much on the number of occupied orbitals. We find that eight to ten occupied orbitals per CPU are needed to obtain a reasonable speedup.

To demonstrate the applicability of the implementation to larger systems, we chose the 7-, 9-, and 11-ring helicenes which are of special interest for second-order property calculations in general due to their chirality. The geometries have been optimized at the MP2/cc-pVTZ level and the polarizability calculations have been done with MP2 and CC2 in the aug-cc-pVTZ basis set. The core orbitals have been kept frozen. The results of the calculations are listed in Table IV. The polarizability increases per benzene ring by about 40 a.u. with

Downloaded 21 Sep 2012 to 134.147.252.238. Redistribution subject to AIP license or copyright; see http://jcp.aip.org/about/rights_and_permissions

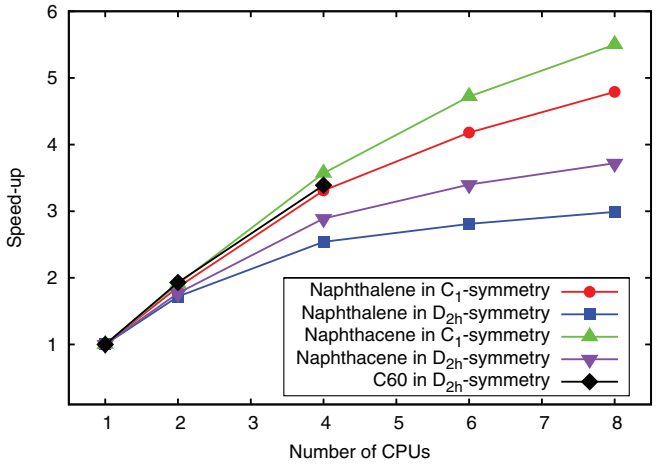


FIG. 3. Parallelization of orbital-unrelaxed CC2 polarizability calculations on C_{60}, Naphthacene, and Naphthalene with and without symmetry. All calculations were done in the aug-cc-pVTZ basis and with frozen core approximation.

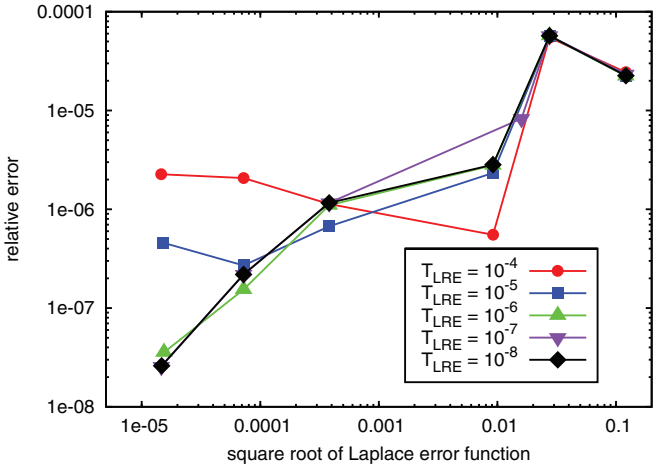


FIG. 4. Change of the Laplace and convergence error in $\alpha_{\max}$ of naphthacene upon variation of T_{LRE} and $\sqrt{F^{\mathrm{Lap}}}$. For $\sqrt{F^{\mathrm{Lap}}} < 0.0004$, the points for $T_{\mathrm{LRE}} = 10^{-7}$ and 10^{-8} are on top of each other.

MP2 and by about 45 a.u. with CC2. With both methods, the increase of the polarizability from 9- to 11-helicene is slightly larger than from 7- to 9-helicene. Since orbital-unrelaxed CC2 is known to overestimate polarizabilities, the MP2 result is expected to be more accurate.

B. Accuracy of the numerical Laplace transformation

The sampling points θ_m for the numerical Laplace transformation are obtained by minimizing the Laplace error functional[30]

$$F^{\mathrm{Lap}}(\theta_m, \omega_m) = \int_{\epsilon_{\min}}^{\epsilon_{\max}} \left(\frac{1}{x} - \sum_{m}^{N_m} \omega_m e^{-x\theta_m} \right)^2 dx, \qquad (53)$$

where $\epsilon_{\min}$ and $\epsilon_{\max}$ are two times the minimum and the maximum difference between any virtual and occupied orbital energy, respectively. F^{Lap} is related to the error of the numerical Laplace transformation. The optimization of the grid points θ_m and weights ω_m by minimization of F^{Lap} are described in Ref. 30.

To study the additional error caused by the numerical Laplace transformation—in the following referred to as Laplace error—we have done calculations on three aromatic molecules and compared the error in the polarizability with F^{Lap}. We have, in particular, been interested in a simple rule for choosing the maximum value of F^{Lap} such that the Laplace error is at most of the same order of magnitude as the error due to the limited convergence of the linear equations for the first-order response of the cluster amplitudes t^x. The latter is determined by the requirement that

$$||(\mathbf{A}^{\mathrm{eff}} - \omega\mathbf{1})t^x - \xi^{x,\mathrm{eff}}|| \leq T_{\mathrm{LRE}}, \qquad (54)$$

where T_{LRE} is a user-specified threshold. We varied for this study both F^{Lap} and T_{LRE} and investigated the relative error in the largest tensor component in a coordinate system where the dipole polarizability tensor is diagonal. This tensor component is in the following denoted as $\alpha_{\max}$. The error has been evaluated as difference to a rigidly converged result which has been computed with F^{Lap} smaller than 10^{-15}. These calculations have been done with orbital-unrelaxed CC2 in the aug-cc-pVTZ basis using the frozen core approximation.

Fig. 4 shows the results for the naphthacene molecule. Similar plots for *p*-nitroaniline and thiophene are included in the supplementary material.[28] Our study shows that the Laplace error is already small for large values of $\sqrt{F^{\mathrm{Lap}}}$. Already at the largest values for $\sqrt{F^{\mathrm{Lap}}}$ (which corresponds to only two sampling points), the error is below 1%. In Fig. 4, the series for $T_{\mathrm{TRE}} \leq 10^{-6}$ shows an approximately linear behavior between $\sqrt{F^{\mathrm{Lap}}} \leq 10^{-6}$ and 0.01 which indicates that the error is dominated by the Laplace error. For the series with $T_{\mathrm{LRE}} = 10^{-5}$ and larger, we observe two regimes: for low

TABLE IV. Results for polarizability calculations on helicene molecules. N_m denotes the number of Laplace sampling points, while α is the isotropic average of the dipole polarizability. All calculations were carried out on 12 Intel(R) Xeon(R) X5670 CPUs with 2.93 GHz. The CPHF equations for the MP2 calculations were solved with exact four-index ERIs after a preoptimization using the RI approximation.

	No. basis funct.			Relaxed MP2		unrelaxed CC2	
Molecule	MO	auxiliary	N_m	α (a.u.)	calc. time (d)	α (a.u.)	calc. time (d)
7-helicene	1794	4008	7	357	2.7	382	3.1
9-helicene	2254	5040	7	437	5.6	470	9.4
11-helicene	2714	6072	7	518	17.7	560	26.4

Downloaded 21 Sep 2012 to 134.147.252.238. Redistribution subject to AIP license or copyright; see http://jcp.aip.org/about/rights_and_permissions

TABLE V. Relative errors in the polarizabilities due to limited convergence of the response equations and the numerical Laplace transformations for different thresholds T_{LRE} and $\sqrt{F^{Lap}} = 100 \cdot T_{\mathrm{LRE}}$.

Molecule	$T_{\mathrm{LRE}} = 10^{-4}$ $\Delta\alpha_{\max} = 2 \times 10^{-4}$	$T_{\mathrm{LRE}} = 10^{-3}$ $\Delta\alpha_{\max} = 2 \times 10^{-3}$
Naphthacene	3.27E-005	2.07E-005
Anthracene	3.04E-006	3.15E-005
Hexafluorobenzene	2.25E-005	1.22E-004
Fluorobenzene	2.45E-006	2.05E-004
Cyclohexane	3.13E-006	3.46E-004
CF_3Br	1.42E-006	1.84E-005
CH_3Cl	9.73E-006	4.28E-004

values of $\sqrt{F^{\mathrm{Lap}}}$, the curves have a flat region where the error is controlled by T_{LRE}, while beyond a certain turnover point, the error increases approximately linear with $\sqrt{F^{\mathrm{Lap}}}$. In summary, we get an upper bound for the relative error of

$$\Delta\alpha_{\max} \leq T_{\mathrm{LRE}} + 0.01\sqrt{F^{\mathrm{Lap}}}. \tag{55}$$

The contribution of the Laplace error is about two orders of magnitude smaller than the error caused by the residual of the response equations. A similar equation was found in a recent study[35] on two-photon absorption strengths, although there the prefactor of $\sqrt{F^{\mathrm{Lap}}}$ was significantly larger since in the calculation of two-photon absorption matrix elements, the Laplace transformation is not only used in density calculations but also for setting up the right-hand-side vectors for the response of Lagrangian multipliers.

To test the relation in Eq. (55), further we have done calculations on different molecules with pairs of $\sqrt{F^{\mathrm{Lap}}}$ and T_{LRE} with $\sqrt{F^{\mathrm{Lap}}} = 100 \cdot T_{\mathrm{LRE}}$ evaluated the relative deviation from tightly converged results ($\sqrt{F^{\mathrm{Lap}}} = 10^{-9}$, $T_{\mathrm{LRE}} = 10^{-6}$). The results listed in Table V show that the relative deviation is in most cases even one or two orders of magnitude below the upper bound $\Delta\alpha_{\max}$.

C. RI and one-electron basis set error

As outlined above the correlation contributions to the polarizabilities are calculated using the RI approximation for the two-electron integrals, while for the solution of the CPHF equations for $\bar{\kappa}$ and κ^x, we can either use exact four-index integrals or also the RI approximation. For the latter case, we choose to expand the two-electron integrals in the same auxiliary basis as used for the correlation contributions. The two algorithms scale different with the size of the basis set and the number of atoms. With four-index ERIs, the computational costs have a large prefactor and scale as $\mathcal{O}(\mathcal{M}^4)$ with the basis set size $\mathcal{M}$, but integral screening eventually leads to a $\mathcal{O}(\mathcal{N}^2)$-scaling with the system size for large molecules. The RI algorithm, on the other hand, scales as $\mathcal{O}(\mathcal{N}^4)$ with a smaller prefactor than the algorithm with four-index ERIs, but has only an $\mathcal{O}(\mathcal{M}^3)$ scaling with the basis set size. Therefore, it is more efficient for medium-sized molecules and for basis sets with diffuse functions, where the integral screening is not efficient.

The RI approximation, however, introduces an additional RI error. To investigate this error, we used a test set of molecules (see supplementary material[28]) which covers the groups III–VIII elements of the first and the second long row of the periodic table. The geometries have been optimized at the RI-MP2/cc-pVTZ level. For these molecules, we have done orbital-relaxed MP2 calculations for the complete dipole polarizability tensors with several augmented correlation consistent basis sets[32,33,36] and the corresponding optimized auxiliary basis sets.[34] The calculations were carried out using both exact four-index ERIs and the RI approximation to solve the CPHF equations. In addition we computed for the first row elements in the aug-cc-pVDZ and aug-cc-pVTZ basis sets reference results without any RI approximation with the CFOUR program package.[37] In all calculations the core orbitals were kept frozen. The results are listed in Table VI. We first note that the RI-CPHF error decreases similar as the RI-MP2 error with the cardinal number of the (auxiliary) basis set. It is also of the same order of magnitude as the latter. The combinations RI-CPHF/RI-MP2 or RI-CPHF/RI-CC2 are thus the methods of choice for the calculation of polarizabilities of medium-sized molecules or when diffuse basis sets are used and integral screening is inefficient.

To study the relevance of the RI error for polarizabilities, we investigated for the same test set the one-electron basis set error. For this, the aug-cc-pVQZ and aug-cc-pV5Z results were extrapolated to the basis set limit using the two-point formula proposed by Helgaker *et al.*[38] which was originally introduced for energies but can also be applied to the

TABLE VI. Mean absolute deviations due to the RI approximation in the MP2 part and the solution of the CPHF equations. The total RI error was calculated as mean absolute deviation between RI-CPHF/RI-MP2 and CPHF/MP2 and the RI-CPHF error as the mean absolute deviation between calculations using four-index ERIs and RI-CPHF for the solution of the CPHF equations. The RI-MP2 error was determined as mean absolute deviation between calculations using MP2 and RI-MP2 for the correlation part, respectively. The listed deviations in the errors are the sample-based standard deviations of the mean absolute deviations.

Basis	RI-CPHF error	RI-MP2 error	total RI error
aug-cc-pVDZ	$6 \times 10^{-5} \pm 8 \times 10^{-5}$	$8 \times 10^{-5} \pm 9 \times 10^{-5}$	$1 \times 10^{-4} \pm 1 \times 10^{-4}$
aug-cc-pVTZ	$7 \times 10^{-6} \pm 1 \times 10^{-5}$	$2 \times 10^{-5} \pm 2 \times 10^{-5}$[a]	$2 \times 10^{-5} \pm 2 \times 10^{-5}$[a]
aug-cc-pVQZ	$4 \times 10^{-6} \pm 1 \times 10^{-5}$		
aug-cc-pV5Z	$3 \times 10^{-7} \pm 5 \times 10^{-6}$		

[a]Only including the compounds with only first row elements without C_6H_6 and $B_3N_3H_6$.

Downloaded 21 Sep 2012 to 134.147.252.238. Redistribution subject to AIP license or copyright; see http://jcp.aip.org/about/rights_and_permissions

TABLE VII. Average one-electron basis set errors in dipole-dipole polarizabilities. The errors in the given values are standard deviations.

Basis set	Basis set error
aug-cc-pVDZ	$7 \times 10^{-2} \pm 2 \times 10^{-1}$
aug-cc-pVTZ	$2 \times 10^{-2} \pm 1 \times 10^{-1}$
aug-cc-pVQZ	$2 \times 10^{-3} \pm 3 \times 10^{-3}$
aug-cc-pV5Z	$1 \times 10^{-3} \pm 1 \times 10^{-3}$

correlation contribution to polarizabilities,

$$\alpha_X = \alpha_{\text{lim}} - A \cdot X^{-3}, \tag{56}$$

where α_X and α_{lim} denote the correlation contributions to the polarizability in the aug-cc-pVXZ basis and at the basis set limit. The estimated limit of the correlation contribution α_{lim} was then combined with the HF result in the aug-cc-pV5Z basis. The average basis set errors with respect to the so-estimated limits are listed in Table VII. They are, in general, several orders of magnitude larger than the RI errors, similar as it has been observed before for other molecular properties calculated with RI-CC2 and RI-MP2.[21]

D. Comparison with experimental data

To explore the accuracy of the implemented methods, in particular CC2, we set up a test set of 29 molecules for which experimental polarizability data are available. For these molecules, we calculated the isotropic polarizabilities using orbital-unrelaxed CC2 as well as orbital-relaxed MP2 and CC2. All calculations were done using the aug-cc-pVTZ orbital[32,33] and auxiliary[34] basis sets and applying the frozen core approximation. A comparison of the results for static polarizabilities with the experimental data is listed in Table VIII. The experimental values taken from Refs. 39 and 40 have been obtained from refractive indices by extrapolation to the static limit and from dipole(e,e)-differential oscillator strength spectroscopy, respectively, and therefore should not contain vibrational contributions so that they are directly comparable to calculated electronic polarizabilities. The experimental value for C_{60} has, however, been measured by deflection of a molecular beam and therefore includes the vibrational contribution.

Comparing the polarizability values for unrelaxed CC2, relaxed MP2, and relaxed CC2, we find that unrelaxed CC2 gives the largest values in all cases, while the relaxed CC2 and MP2 results are lower. The results from relaxed CC2 are always slightly higher than the relaxed MP2 values. This is in line with several previous studies which point out that CC2 has a tendency to overestimate polarizabilities.[14,15,42,43] The results in Table VIII also show that for acyclic compounds the MP2 values are often slightly lower than experiment, while for aromatic compounds the polarizabilities are overestimated by all methods. The largest deviations

TABLE VIII. Static polarizability data from calculation and experiment. All values are given in atomic units.

Molecule	No.	CC2 unrelaxed	MP2 relaxed	CC2 relaxed	Expt.
Ethane	1	28.9	28.2	28.4	29.7 (Ref. 39)
Propane	2	41.3	40.2	40.5	39.96 (Ref. 40)
Butane	3	53.8	52.3	52.7	51.88 (Ref. 40)
Pentane	4	66.4	64.5	65.0	64.64 (Ref. 40)
Hexane	5	79.1	77.8	77.5	77.25 (Ref. 40)
Heptane	6	91.9	89.2	90.0	89.67 (Ref. 40)
Octane	7	104.7	101.6	102.7	100.7 (Ref. 40)
Ethene	8	27.9	27.2	27.4	27.6 (Ref. 39)
Allene	9	41.7	40.0	40.5	40.5 (Ref. 39)
But-2-yne	10	50.0	48.9	49.2	50.5 (Ref. 39)
Cyclopropane	11	37.2	36.1	36.4	38.1 (Ref. 39)
Cyclohexane	12	72.6	70.1	70.8	72.54 (Ref. 39)
CH_3F	13	17.4	16.7	17.0	17.7 (Ref. 39)
CH_3Cl	14	29.9	29.1	29.3	30.0 (Ref. 39)
CCl_4	15	72.3	69.1	70.0	67.5 (Ref. 40)
CH_3Br	16	37.3	36.2	36.3	37.5 (Ref. 39)
CF_3Br	17	40.0	37.9	38.7	38.1 (Ref. 39)
Methanol	18	21.9	21.0	21.4	20.79 (Ref. 40)
Formaldehyde	19	18.6	17.6	18.0	18.69 (Ref. 40)
Acetaldehyde	20	31.6	30.0	30.7	28.87 (Ref. 40)
Acetone	21	43.6	41.6	42.4	41.14 (Ref. 40)
Dimethylamine	22	39.2	37.8	38.4	36.76 (Ref. 40)
Trimethylamine	23	53.0	50.5	51.8	47.75 (Ref. 40)
Methylamine	24	26.4	25.6	25.9	25.33 (Ref. 40)
Benzene	25	71.4	69.1	69.4	67.2 (Ref. 39)
Fluorobenzene	26	71.9	68.9	69.7	66.5 (Ref. 39)
Hexafluorobenzene	27	76.9	71.5	73.6	66.3 (Ref. 39)
Naphthalene	28	124.3	118.7	120.8	117.4 (Ref. 39)
C_{60}	29	623.7	559.6	571.9	516.2 (Ref. 41)

Downloaded 21 Sep 2012 to 134.147.252.238. Redistribution subject to AIP license or copyright; see http://jcp.aip.org/about/rights_and_permissions

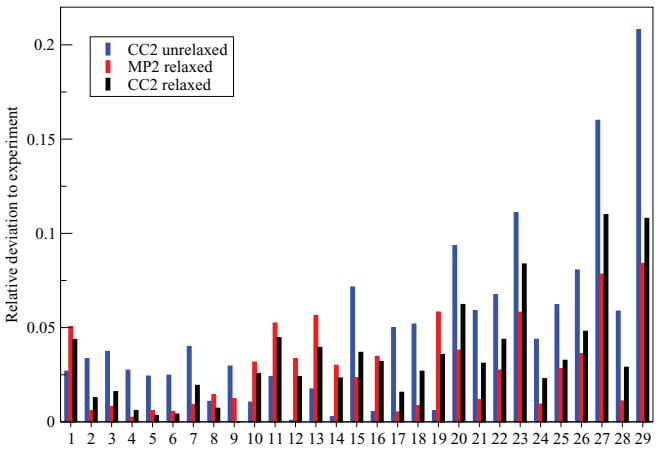


FIG. 5. Relative errors to the experimental values for the results in Table VIII. The numbers of the molecules are the same as in Table VIII.

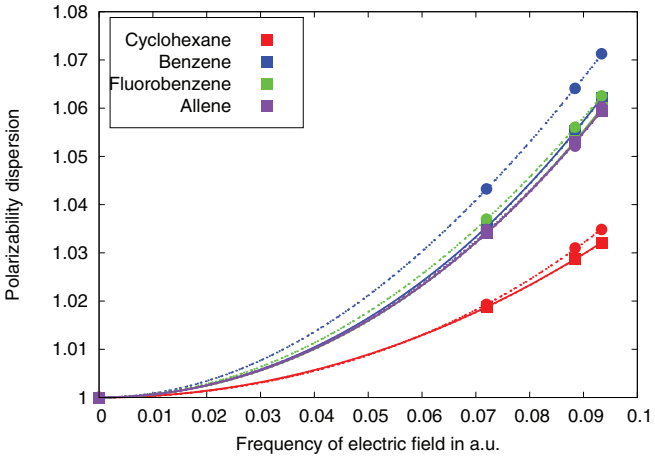


FIG. 6. Polarizability dispersion in cyclohexane, benzene, fluorobenzene, and allene. Dots and solid lines denote calculated values from CC2, while squares and dotted lines denote experimental values. Note that the two lines for allene are on top of each other and they also cover the solid line for fluorobenzene.

between calculated and experimental results are found for hexafluorobenzene, fluorobenzene, and C_{60}. The best agreement with experimental results is, in general, obtained with orbital-relaxed MP2 which we recommend for static polarizability calculations. This is in line with the findings in Ref. 44. From Fig. 5, it can be seen that all relative deviations are in the range of a few percent or lower for MP2, while for relaxed and unrelaxed CC2, some of the relative deviations are larger than 10%. For C_{60}, Kowalski and coworkers[45] reported recently a result of 555.25 a.u. obtained with CCSD in the ZPolC basis set which is only slightly below the MP2 but significantly below CC2 result in the aug-cc-pVTZ basis.

Since orbital-relaxed CC2 and MP2 have unphysical pole structures due to the presence of poles both from the Hartree-Fock and the correlated calculation, they give unreliable results for frequency-dependent polarizabilities. In this case, orbital-unrelaxed CC2 is the preferred approach. We used this method to calculate the dispersion of the polarizability of several molecules. In earlier studies, CC2 was shown to offer a significant improvement for the dispersion of frequency-dependent polarizabilities compared to Hartree-Fock and coupled cluster singles (CIS).[46] In Table IX, the results are compared with experimental data. For some molecules, plots of the polarizability dispersion are shown in Fig. 6, which show that the experimental dispersion can excellently be reproduced by CC2.

For but-2-yne, the experimental frequency-dependent values are lower than the static values (see Table VIII) which are unphysical for frequencies below the first excitation energy. Also for cyclopropane and hexafluorobenzene, the experimental static values from Ref. 39 do not seem to fit together with the frequency-dependent values from Ref. 47 on a physically meaningful curve. Therefore, for these molecules, we do not analyze the dispersions but the ratios between the polarizability values at the different wavelength with the value at 633 nm being set to 1. These ratios are listed in Table X.

TABLE IX. Frequency-dependent polarizabilities (in a.u.) for some organic molecules from unrelaxed CC2 calculations, from a combination of relaxed MP2 with the unrelaxed CC2 dispersion (α^{Comb}) and experiment (Expt.). Experimental data are from Ref. 47 if not stated otherwise. Apart from C_{60}, which was measured by a light force technique, all experimental data are from refractive index measurements. [48]

Wavelength (nm)	488			515			633		
Molecule	CC2	α^{Comb}	Expt.	CC2	α^{Comb}	Expt.	CC2	α^{Comb}	Expt.
Ethene	29.2	28.5	28.99	29.1	28.4	28.87	28.7	28.0	28.51
Allene	56.3	54.0	42.94	55.6	53.4	42.64	53.7	51.5	41.91
Cyclopropane	38.4	37.3	38.70	38.3	37.2	38.51	37.9	36.8	38.11
But-2-yne	52.0	50.9	50.46	51.8	50.7	50.28	51.1	50.0	49.67
Cyclohexane	74.9	72.4	75.21	74.7	72.1	74.60	74.0	71.4	73.99
Benzene	75.8	73.4	71.99	75.3	72.9	71.51	73.9	71.5	70.11
Fluorobenzene	76.2	73.0	70.66	75.7	72.6	70.23	74.3	71.3	68.96
Hexafluorobenzene	80.8	75.1	71.99	80.4	74.7	71.69	79.2	73.6	70.66

Wavelength (nm)	1064		
Molecule	CC2	$\alpha^{\text{Comb.}}$	Exp.
C_{60}	641.0	575.2	533.12 (Ref. 49)

Downloaded 21 Sep 2012 to 134.147.252.238. Redistribution subject to AIP license or copyright; see http://jcp.aip.org/about/rights_and_permissions

TABLE X. Ratios between frequency-dependent polarizabilities for cyclopropane, but-2-yne, and hexafluorobenzene.

Ratio	α_{488}: α_{633}		α_{515}: α_{633}	
Molecule	CC2	Expt.	CC2	Expt.
Cyclopropane	1.0137	1.0155	1.0103	1.0105
But-2-yne	1.0164	1.0159	1.0121	1.0123
Hexafluorobenzene	1.0211	1.0188	1.0157	1.0146

Evaluating these data we find that especially for but-2-yne, there is an excellent agreement between experimental and calculated values.

Orbital-relaxed MP2 performs well for static polarizabilities and unrelaxed CC2 describes accurately the dispersion. This suggests to combine the advantages of these two approaches by scaling the static orbital-relaxed MP2 result with the dispersion from unrelaxed CC2:

$$\alpha^{\mathrm{Comb}}(\omega) = \alpha_{\mathrm{MP2,rel}}(0) \cdot \frac{\alpha_{\mathrm{CC2,unrel}}(\omega)}{\alpha_{\mathrm{CC2,unrel}}(0)}. \tag{57}$$

The results for α^{Comb} have been included in Table IX. Especially for the aromatic molecules and C_{60}, α^{Comb} reproduces experimental values significantly better than CC2 itself, while for ethane, ethene, cyclopropane, and cyclohexane, no improvement is seen since for these molecules, the unrelaxed CC2 values are already close to the experimental values. Concerning C_{60} we also note that α^{Comb} at 1064 nm is in quite good agreement with the CCSD results of 564.85 a.u. obtained by Kowalski *et al.* for this wavelength,[45] it is only 10 a.u. or 2% higher.

V. CONCLUSIONS

We have presented an implementation of dipole polarizabilities for CC2 and MP2 which used the RI approximation for two-electron integrals. This is, to our knowledge, also the first implementation of RI-MP2 for second-order properties. By using the RI approximation and a numerical Laplace transformation, storage of $\mathcal{O}(\mathcal{N}^4)$-scaling arrays could be avoided which reduces significantly the disc space demands. Even molecules with more than 2000 basis functions can be treated in about a day's time on standard computer hardware using point group symmetry and a shared memory parallelization. This allowed large scale applications on helicene molecules with up to 11 rings and more than 2700 basis functions. 11-helicene and C_{60} are, to our knowledge, the largest systems for which second-order properties have ever been studied with coupled cluster theory. For static polarizabilities, orbital-relaxed MP2 reproduces experimental values within a few percent and is the recommended second-order wave function method for the calculation of static polarizabilities of large molecules if a high accuracy is needed. For unrelaxed and orbital-relaxed CC2, the deviations are larger. Orbital relaxation causes, however, problems for frequency-dependent properties. Unrelaxed CC2 reproduces the experimental dispersion curves of polarizabilities very well with only small drifts which depend on the errors in the excitation energies for the lowest dipole-allowed transitions. An additional improvement of frequency-dependent polarizabilities has been realized by the combination of orbital-relaxed MP2 calculations with the dispersion from unrelaxed CC2.

The presented implementation for polarizabilities is an important keystone both for a generalization to excited state second-order properties (relaxed and unrelaxed) as well as for the implementation of ground state properties which involve derivatives of the atomic orbitals not taken into account here. It paves, in particular, the way for the implementation of force constants and dipole gradients which are needed, e.g., for vibrational frequencies and infra-red intensities. Work in this direction is in progress.

ACKNOWLEDGMENTS

The authors acknowledge support by the Deutsche Forschungsgemeinschaft (DFG) through Grant No. HA 2588/5-1. D.H.F also acknowledges the financial support by the Studienstiftung des Deutschen Volkes through a PhD scholarship.

[1] J. F. Stanton and J. Gauss, Int. Rev. Phys. Chem. **19**, 61 (2000).
[2] J. P. Merrick, D. Moran, and L. Radom, J. Phys. Chem. A **111**, 11683 (2007).
[3] S. J. A. van Gisbergen, J. G. Snijders, and E. J. Baerends, J. Chem. Phys. **103**, 9347 (1995).
[4] S. A. McDowell, R. D. Amos, and N. C. Handy, Chem. Phys. Lett. **235**, 1 (1995).
[5] B. Champagne, E. A. Perpète, S. J. A. van Gisbergen, E.-J. Baerends, J. G. Snijders, C. Soubra-Ghaoui, K. A. Robins, and B. Kirtman, J. Chem. Phys. **109**, 10489 (1998).
[6] O. Christiansen, H. Koch, and P. Jørgensen, Chem. Phys. Lett. **243**, 409 (1995).
[7] N. Handy, R. Amos, J. Gaw, J. Rice, and E. Simandiras, Chem. Phys. Lett. **120**, 151 (1985).
[8] E. Simandiras, R. Amos, and N. Handy, Chem. Phys. **114**, 9 (1987).
[9] J. E. Rice and N. C. Handy, J. Chem. Phys. **94**, 4959 (1991).
[10] C. Hättig and B. A. Heß, Chem. Phys. Lett. **233**, 359 (1995).
[11] O. Christiansen, A. Halkier, H. Koch, P. Jørgensen, and T. Helgaker, J. Chem. Phys. **108**, 2801 (1998).
[12] M. Kállay and J. Gauss, J. Chem. Phys. **120**, 6841 (2004).
[13] J. Gauss, K. Ruud, and M. Kállay, J. Chem. Phys. **127**, 074101 (2007).
[14] T. Korona, Phys. Chem. Chem. Phys. **12**, 14977 (2010).
[15] T. B. Pedersen, A. M. J. S. Sanchez de Meras, and H. Koch, J. Chem. Phys. **120**, 8887 (2004).
[16] T. Korona, K. Pflüger, and H.-J. Werner, Phys. Chem. Chem. Phys. **6**, 2059 (2004).
[17] R. Chelli and P. Procacci, J. Chem. Phys. **117**, 9175 (2002).
[18] T. Verstraelen, V. V. Speybroeck, and M. Waroquier, J. Chem. Phys. **131**, 044127 (2009).
[19] C. Hättig, J. Chem. Phys. **118**, 7751 (2003).
[20] C. Hättig and F. Weigend, J. Chem. Phys. **113**, 5154 (2000).
[21] C. Hättig and A. Köhn, J. Chem. Phys. **117**, 6939 (2002).
[22] A. Köhn and C. Hättig, J. Chem. Phys. **119**, 5021 (2003).
[23] C. Hättig, O. Christiansen, and P. Jørgensen, J. Chem. Phys. **108**, 8331 (1998).
[24] T. Helgaker and P. Jørgensen, Theor. Chem. Acc. **75**, 111 (1989).
[25] H. Koch, H. J. A. Jensen, P. Jørgensen, T. Helgaker, G. E. Scuseria, and H. F. Schaefer III, J. Chem. Phys. **92**, 4924 (1990).
[26] O. Christiansen, P. Jørgensen, and C. Hättig, Int. J. Quantum. Chem. **68**, 1 (1998).
[27] T. Helgaker, P. Jørgensen, and J. Olsen, *Molecular Electronic Structure Theory* (Wiley, 2000).
[28] See supplementary material at http://dx.doi.org/10.1063/1.4704788 for explicit working equations on two-particle densities, effective fock matrices, the corresponding intermediates, and additional calculated data.

Downloaded 21 Sep 2012 to 134.147.252.238. Redistribution subject to AIP license or copyright; see http://jcp.aip.org/about/rights_and_permissions

[29]Turbomole v6.3 2011, a development of University of Karlsruhe and Forschungszentrum Karlsruhe GmbH, 1989–2007, TURBOMOLE GmbH, since 2007; see http://www.turbomole.com.
[30]N. O.C. Winter and C. Hättig, J. Chem. Phys. **134**, 184101 (2011).
[31]P. Jørgensen and T. Helgaker, J. Chem. Phys. **89**, 1560 (1988).
[32]T. H. Dunning, J. Chem. Phys. **90**, 1007 (1989).
[33]D. E. Woon and T. H. Dunning, J. Chem. Phys. **98**, 1358 (1993).
[34]F. Weigend, A. Köhn, and C. Hättig, J. Chem. Phys. **116**, 3175 (2002).
[35]D. H. Friese, C. Hättig, and K. Ruud, Phys. Chem. Chem. Phys. **14**, 1175 (2012).
[36]R. A. Kendall, J. Thom, H. Dunning, and R. J. Harrison, J. Chem. Phys. **96**, 6796 (1992).
[37]CFOUR, Coupled-Cluster techniques for Computational Chemistry, a quantum-chemical program package by J. F. Stanton, J. Gauss, M. E. Harding, and P. G. Szalay with contributions from A. A. Auer, R. J. Bartlett, U. Benedikt, C. Berger, D. E. Bernholdt, Y. J. Bomble, L. Cheng, O. Christiansen, M. Heckert, O. Heun, C. Huber, T.-C. Jagau, D. Jonsson, J. Jusélius, K. Klein, W. J. Lauderdale, D. A. Matthews, T. Metzroth, L. A. Mück, D. P. O'Neill, D. R. Price, E. Prochnow, C. Puzzarini, K. Ruud, F. Schiffmann, W. Schwalbach, S. Stopkowicz, A. Tajti, J. Vázquez, F. Wang, and J. D. Watts and the integral packages MOLECULE (J. Almlöf and P. R. Taylor), PROPS (P. R. Taylor), ABACUS (T. Helgaker, H. J. Aa. Jensen, P. Jørgensen, and J. Olsen), and ECP routines by A. V. Mitin and C. van Wüllen. For the current version, see http://www.cfour.de.
[38]T. Helgaker, W. Klopper, H. Koch, and J. Noga, J. Chem. Phys. **106**, 9639 (1997).
[39]M. Gussoni, M. Rui, and G. Zerbi, J. Mol. Struct. **447**, 163 (1998).
[40]T. N. Olney, N. Cann, G. Cooper, and C. Brion, Chem. Phys. **223**, 59 (1997).
[41]R. Antoine, P. Dugourd, D. Rayane, E. Benichou, M. Broyer, F. Chandezon, and C. Guet, J. Chem. Phys. **110**, 9771 (1999).
[42]O. Christiansen, A. Halkier, and P. Jørgensen, Chem. Phys. Lett. **281**, 438 (1997).
[43]O. Christiansen, C. Hättig, and P. Jørgensen, Spectrochim. Acta, Part A **55**, 509 (1999).
[44]O. Christiansen, C. Hättig, and J. Gauss, J. Chem. Phys. **109**, 4745 (1998).
[45]K. Kowalski, J. R. Hammond, W. A. de Jong, and A. J. Sadlej, J. Chem. Phys. **129**, 226101 (2008).
[46]C. Hättig and P. Jørgensen, J. Chem. Phys. **109**, 2762 (1998).
[47]M. P. Bogaard, A. D. Buckingham, R. K. Pierens, and A. H. White, J. Chem. Soc., Faraday Trans. 1 **74**, 3008 (1978).
[48]U. Hohm, Chem. Phys. **179**, 533 (1994).
[49]A. Ballard, K. Bonin, and J. Louderback, J. Chem. Phys. **113**, 5732 (2000).

Downloaded 21 Sep 2012 to 134.147.252.238. Redistribution subject to AIP license or copyright; see http://jcp.aip.org/about/rights_and_permissions